

Inverse Gaussian mixtures models of bearing vibrations under local faults

Pavle Boškosi^{a,*}, Đani Juričić^a

^a*Jožef Stefan Institute, Department of Systems and Control, Jamova cesta 39, SI-1000 Ljubljana, Slovenia*

Abstract

Repetitive impacts performed by damaged spot on a component of the rolling element bearing specific statistical properties, due to the constant angular distance between the roller elements. Under (almost) constant rotational speed the successive impacts are regarded as almost periodic with small random fluctuations due to slippage. Often these random components are modelled as normally distributed, which is unrealistic since physically impossible events, such as negative time between two consecutive impacts become likely by the nature of the distribution. Motivated by this deficiency we propose a new model that describes the occurrence of repetitive vibrational patterns as realisation of a point process with the (mixture)inverse Gaussian distribution of the inter-event times. Such a model is applicable to both constant and variable rotational speeds. Additionally, the proposed model inherently describes the quasi-cyclostationarity of the impact times under almost constant rotational speed. The applicability of the model was evaluated using vibrational signals generated by bearings with localised surface fault.

Keywords: Localised surface bearing faults, Inverse Gaussian distribution, Fault modelling, Bayes' factor, Variable rotational speed

1. Introduction

Bearing faults among the most common causes for mechanical failures [1, 2]. Commonly, methods based on analysis of vibrational signals focus on extracting specific frequency components that are linked to particular surface faults [3]. Inferring about bearing condition using such a feature set is possible if the monitored bearing operates under constant and known rotational speed. However, in reality rotational speed fluctuates so that the effectiveness of these features is significantly reduced. In this paper we model the vibrational patterns, generated by bearings with localised surface fault, as a point process with inverse Gaussian mixture inter-event distribution.

The main source of information for detecting localised bearing faults are the time occurrences of particular vibrational patterns. The observation of these repetitive vibrational patterns through the concepts of point

*Corresponding author.

Email addresses: pavle.boskoski@ijs.si (Pavle Boškosi), dani.juricic@ijs.si (Đani Juričić)

processes was firstly proposed by Antoni and Randall [4]. The proposed model was based on a periodic impact occurrences with small variations in the period modelled as Gaussian random variable. In a similar approach Borghesani et al. [5] analysed the distribution of the times between consecutive impacts that emerge under non-stationary but known operating conditions by allowing significant speed variations and by calculating the squared envelope spectrum coupled with computed order tracking. The approach proposed in this paper goes one step further by removing the limitation of constant and known operating conditions.

Despite the effectiveness of the proposed models, they suffer from two major deficiencies. Firstly, the time intervals between two consecutive impacts are modelled as Gaussian random variables. Since the support of the Gaussian distribution is on the interval $(-\infty, \infty)$, it is likely that a time increment takes negative value which is physically impossible. The second deficiency regards the capability of modelling significant speed fluctuations. By incorporating random speed fluctuations one significantly increases the complexity of currently adopted models. Therefore, we propose a novel model that describes the impact occurrences, generated by localised bearing surface damage, as realisation of a point process whose inter-event times are governed by (mixture) inverse Gaussian (IG) distribution. By using such an approach one can construct a unified model capable of describing both single and multiple bearing faults regardless of the speed fluctuations. We have to note that in this paper we do not deal with fault diagnosis itself. However, the diagnostic approach proposed in [6] for a particular instance of the problem treated below is readily applicable for the results derived in this paper.

The paper is organised as follows. The idea of point processes, which are basic building blocks of the model, are presented in Section 2. The definition and essential statistical properties of the inverse Gaussian distribution and its mixture variant are presented in Section 3. Applicability of the proposed framework for modelling localised bearing faults is presented in Section 4. The question of whether to use pure or mixture IG distribution based on Bayes' factor is analysed in Section 5. Finally, the simulated and experimental results are presented in Section 6

2. Basics of point processes

Point processes represent a branch of the theory of random processes that are most commonly used for characterising random collections of point occurrences [7]. In the simplest form, these points usually represent the time instances of their occurrences $\dots, t_{i-1}, t_i, t_{i+1}, \dots$ with the corresponding amplitudes $\dots, A_{i-1}, A_i, A_{i+1}, \dots$, as shown in Figure 1. A point process can be specified in several equivalent ways [8]:

- through the non-negative number $N \in \mathbb{Z}^+$ that specifies the number of observed occurrences within some time interval;
- through the distribution of the inter-event times $\{T_1, \dots, T_n\}$ where $T_i = t_i - t_{i-1}$; and

- through the frequency with which events occur around the time instance t with respect to the history \mathcal{H}_t of the process; this statistical property is usually called conditional intensity function $\lambda(t|\mathcal{H}_t)$.

The amplitudes A_i , on the other hand, can be regarded as independent of event times t_i and are not of interest in this paper.

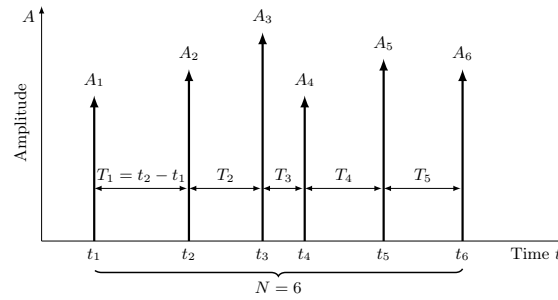


Figure 1: Realisation of a point process

The simplest point process is Poisson process for which the probability of observing k events in a time interval $[0, t]$ follows the Poisson distribution:

$$P(N = k) = \frac{e^{-\lambda t} (\lambda t)^k}{k!}, \quad (1)$$

where the parameter λ is referred to as the intensity of the process. Equivalently, the distribution of the inter-arrival times T_i follows the exponential distribution:

$$p(t) = \lambda e^{-\lambda t}. \quad (2)$$

Finally, for the Poisson process, the intensity function $\lambda(t|\mathcal{H}_t)$ is constant $\lambda(t|\mathcal{H}_t) = \lambda$ and is independent of the history of previous events. In the remaining of the paper, we will use abbreviated notation for probability distribution function (PDF) $p(x)$ instead of $p_X(X = x)$, meaning the PDF of the random variable X takes value x .

The concept of point processes can be applied to describe the impact time occurrences typical for bearings with localised surface faults. In what follows, a point process whose inter-arrival times follow IG distribution is analysed for the purpose of describing localised surface bearing faults.

3. Pure and mixed inverse Gaussian distributions

In this section we will first highlight the basics of a point process with IG distributed inter-arrival times and will provide physical background leading to IG distribution. Additionally, a modification of the original distribution, the so-called mixture IG distribution, with time-varying parameters is presented. Such a concept allows for extension of the proposed localised faults model for bearings operating under variable rotational speed.

3.1. Pure inverse Gaussian distribution

Let a stochastic process $\alpha(t)$ be

$$\alpha(t) = \nu t + \sigma^2 W(t), \quad \nu > 0, t > 0 \tag{3}$$

where ν is positive drift, σ^2 is variance and $W(t)$ is Wiener process with $W(0) = 0$ and with increments $W(t) - W(s) \sim \mathcal{N}(0, t - s)$ [9]. Let us define two parameters:

$$\mu = \frac{a}{\nu} \text{ and } \lambda = \frac{a^2}{\sigma^2}, \tag{4}$$

where the parameter a is a fixed constant. A simple realization of such a process is shown in Figure 2.

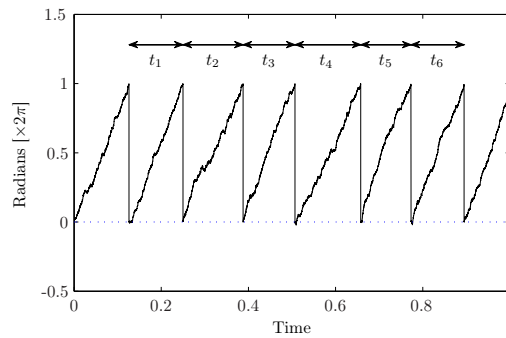


Figure 2: Simulated realisation of the stochastic process (3). The time intervals t_i are distributed by inverse Gaussian distribution (5)

Schrödinger [10] showed that the first passage time of the process (3) over a fixed threshold a follows the inverse Gaussian (IG) distribution $t \sim IG(\mu, \lambda)$ [11]:

$$p(t; \mu, \lambda) = \sqrt{\frac{\lambda}{2\pi t^3}} \exp\left(-\frac{\lambda(t - \mu)^2}{2\mu^2 t}\right), \quad t > 0. \tag{5}$$

Since the parameters μ and λ in (5) are time invariant, the resulting stochastic process is stationary. IG distributions for different values of μ and λ are shown in Figure 3

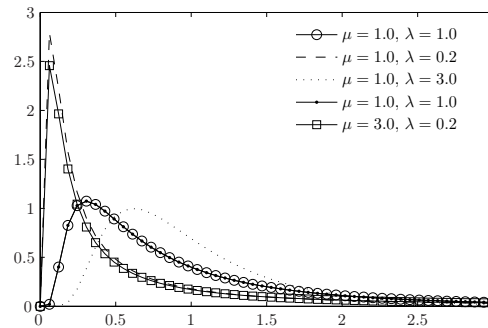


Figure 3: Inverse Gaussian distribution

3.2. Mixed inverse Gaussian distribution

When modelling data generated by Wiener process (3) there are many practical situations in which parameters μ and λ are uncertain and should be considered as random variables, which lead to the so-called inverse Gaussian mixtures [12]. Physically more sound is to allow the positive drift ν in (3) to vary randomly according to some pre-defined distribution. In order to keep the relation with the positive drift ν more clearly visible, Desmond and Chapman [13] re-parametrized (5) by setting $\delta = 1/\mu$:

$$p(t; \delta, \lambda) = \sqrt{\frac{\lambda}{2\pi t^3}} \exp\left(-\frac{\lambda(\delta t - 1)^2}{2t}\right). \quad (6)$$

In such a form the parameter δ is linearly related to the positive drift ν in (3). By allowing δ to be random variable defined on \mathbb{R}^+ with distribution $p_\delta(\delta)$, the marginal distribution reads:

$$p(t; \lambda) = \int_{\delta \in \mathbb{R}^+} p(t; \lambda|\delta)p(\delta) d\delta. \quad (7)$$

4. Modelling localised bearing faults by means of inverse Gaussian models

Localised bearing faults are surface damages that occur on the bearing elements. Each time a rolling element passes over the damaged spot, a specific vibrational pattern is generated. These patterns are directly connected to the bearing's impulse response. Usually, under constant operating conditions the generated vibrations are modelled as [14]:

$$x(t) = \sum_i A_i s(t - iT - \tau_i) + n(t), \quad (8)$$

where A_i is the amplitude of the i^{th} impact, $s(t)$ is the bearing's impulse response, T is the period of rotation, τ_i is random fluctuation mainly to accommodate slippage and small speed fluctuations and $n(t)$ is additive noise. Generally, τ_i is modelled as zero mean normally distributed random variable with sufficiently small variance σ_τ^2 . In such a case τ_i might take negative values, which (theoretically) can even exceed the period of rotation T . Such a scenario, possible in theory, is impossible in practice.

In order to avoid the issues of negative time delays, present in the model (8), we modify the model by taking into account some mechanical properties of the bearings. The angular distance between the adjacent rolling elements is constant and therefore the angular distance between two consecutive impacts can be regarded as constant too. So, one can easily apply the stochastic process (3) to model the angular distance traveled by a rolling element with respect to the damaged spot. The threshold a in (3) is the actual angular distance between the roller elements and ν is directly related to the rotational speed. Consequently, the time intervals between two adjacent excitations of $s(t)$ can be modelled as a realisation of either pure or mixture inverse Gaussian, depending on the statistical characteristics of the rotational speed.

Based on these arguments, we propose the following model of the generated vibrations [14]:

$$x(t) = \sum_i A_i s(t - t_i) + n(t), \quad (9)$$

where A_i is the amplitude of the i th impact, $s(t)$ is the bearing's impulse response and t_i is the time of occurrence modelled as pure or mixture inverse Gaussian random variable and $n(t)$ is additive noise. A typical vibrational pattern is illustrated in Figure 4.

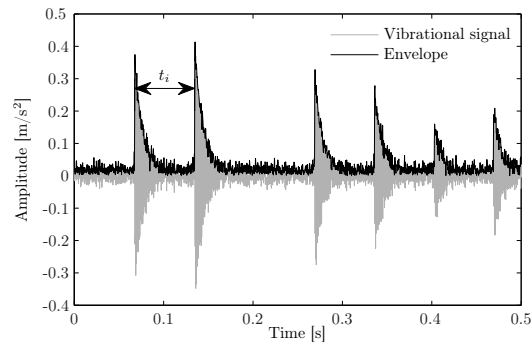


Figure 4: Simulated vibrational pattern generated by damaged bearing

Pure inverse Gaussian model (5) for the inter-impact times t_i should be regarded as a special case, valid when the bearing rotational speed is (almost) constant, meaning there are no significant speed fluctuations [15].

A more realistic scenario is the one where the rotational speed of a bearing varies randomly. Under such circumstances the angle travelled by a rolling element can be modelled as a realisation of the stochastic process (3) by allowing positive drift ν to vary randomly according to the random speed fluctuations. Consequently, the observed time intervals t_i between two consecutive impacts can be modelled as realisation of an inverse Gaussian mixture (7) [16].

In order to show the applicability of the proposed model for localised bearing faults, several scenarios have to be analysed:

- single localised fault present on various bearing elements,
- multiple localised bearing faults and
- statistical properties of the generated vibrational patterns under constant and variable rotating speed.

4.1. Single bearing fault

Crucial information in the analysis of bearing faults is the shaft speed. The shaft speed directly influences the angle evolution of the rolling elements $\alpha(t)$, with respect to a particular bearing component [3]. In context of relation (3), the positive drift ν is related to the shaft's rotational speed through a multiplying parameter C_k . This parameter depends on the geometrical characteristics of the bearing and determines the ratio between the angular speed of the rotating ring and a specific bearing component, i.e. $k \in \{\text{Inner ring, Outer Ring, Bearing Cage, Ball spin}\}$. Consequently, localised surface bearing faults can be represented by

a point process with inter-event intervals distributed by Inverse Gaussian distribution with $\nu = C_k \nu_{shaft}$. The distribution of the inter-event times for the k th component reads:

$$t_k \sim IG \left(\frac{a}{C_k \nu_{shaft}}, \frac{a^2}{\sigma^2} \right), \quad (10)$$

where a is the angular distance between the roller element and the localised fault and σ is the angle variation introduced by slippage. Relation (10) shows that a single localised bearing fault will induce impacts with inter-event times distributed by inverse Gaussian distribution, regardless of the location of the damaged spot.

4.2. Multiple localised faults

The case of multiple localised surface faults can also be described in the framework of point processes with inverse Gaussian inter-event distribution. For that purpose one can consider a Wiener process, similar to (3), with two thresholds a and b . Starting from an initial point the time required to reach the threshold a is T_1 , and time to reach the threshold b from a is T_2 . Based on the results from Chhikara and Folks [17], one can show that T_1 and T_2 are independent inverse Gaussian random variables defined by:

$$\begin{aligned} T_1 &\sim IG \left(\frac{a}{\nu}, \frac{a^2}{\sigma^2} \right) \\ T_2 &\sim IG \left(\frac{b-a}{\nu}, \frac{(b-a)^2}{\sigma^2} \right) \end{aligned} \quad (11)$$

After starting from the initial point, the threshold b is reached at time $T_3 = T_1 + T_2$. Since the ratio

$$\frac{\lambda_i}{\mu_i^2} = \frac{\nu^2}{\sigma^2} = \text{const.}, \quad (12)$$

the time T_3 is also inverse Gaussian random variable distributed as [17]:

$$T_3 \sim IG \left(\mu_1 + \mu_2, \frac{\nu^2(\mu_1 + \mu_2)^2}{\sigma^2} \right). \quad (13)$$

In the context of bearings, the threshold a is the angular distance between the first damaged spot and some initial point, measured in the direction of rotation. The threshold b , on the other hand, is the angular distance between the second and the first damaged spot in the direction of rotation, as shown in Figure 5. By extending the concept of two thresholds (13) to multiple thresholds, one can model multiple localised bearing faults by employing the generalised distribution of inter-event times [17, Chapter 11].

4.3. (Pseudo) Cyclostationarity vibrations at (almost) constant rotating speed

In an idealised case, with strictly constant rotating speed and no slippage, the distribution of the time impacts t_k , described by (10), reduces to $p(t; \nu, \sigma = 0) = \delta(\nu t - a)$, where $\delta(\cdot)$ stands for Dirac δ -function. Consequently, the corresponding point process will be transformed into a truly periodic sequence of impacts.

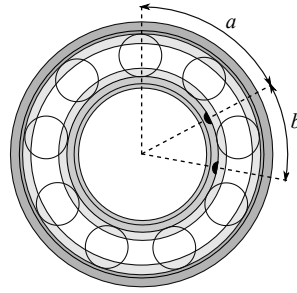


Figure 5: Multiple localised bearing faults

The inherent slippage can be accommodated by allowing small values of σ in (5). The autocorrelation function of the stationary renewal process (9) with $t_i \sim IG(\nu, \sigma)$ can be derived through its inter-event probability distribution [18]. Using (5) as inter-event probability distribution it can be readily shown that the autocorrelation function converges to the constant value

$$\lim_{\tau \rightarrow \infty} R_{xx}(\tau) = \frac{2\sigma^2}{a\nu} < \infty. \tag{14}$$

The details about the derivation of (14) are presented in Appendix A.

As already analysed by Antoni and Randall [19], such a process can be treated as quasi-cyclostationary in cases when σ is sufficiently small and constant rotational speed.

4.4. Fluctuations of impact times

In the simplest form, with constant positive drift ν (constant rotational speed), the variance of the inter-impact times can be derived from the inverse Gaussian distribution (5) as

$$Var[t] = E[(t - E[t])^2] = \frac{\mu^3}{\lambda} = \frac{a\sigma^2}{\nu^3}. \tag{15}$$

The variance (15) depends only on the rotational speed (i.e. the positive drift ν) and is therefore constant over time. For randomly varying speed, the variance of impact times depends on the statistical properties of the rotational speed i.e. the prior $p_\delta(\delta)$ in (7).

4.5. Comments on the model

In the proposed approach the angle evolution of the bearing roller element is modelled as a Wiener process with positive drift (3). In theory, the Wiener process anticipates increments that are not necessarily positive. This property raises two questions:

1. What does negative evolution of the angle $\alpha(t)$ travelled by the rolling element mean?

The slippage causes the roller elements to actually have a negative angle increment relatively to the rotating ring, which on a very short scale is a sort of back and forth movement. The non-monotonic nature of the Wiener process (3) accommodates this effect.

2. What does it mean that a rolling element has a possibility of entering the damaged area several consecutive times?

As a result of the negative angle evolution, there is a (negligible) probability for a rolling element to enter a damaged area more than ones. However, even if such an event occurs, the time between two consecutive impacts will be so short, that on the macroscopic level the first impulse response will be interlaced with the second one and both impacts will become indistinguishable.

By clarifying these two issues the application of the Wiener process (3) becomes physically justified. Furthermore, having a proper statistical model describing the time evolution, one can easily calculate the probability of negative evolution of $\alpha(t)$.

5. Choosing between pure and mixture inverse Gaussian models

The likelihood functions (5) and (7) specify two different models M_1 and M_2 describing the time occurrences t in (9). For these cases when precise rotational speed measurements are available, selecting the proper model is straightforward. However in cases when such measurements are unavailable, a general purpose decision approach can be performed by employing Bayes' factor.

The application of the Bayes' factor incorporates the concepts of parsimony, unlike the standard likelihood which suffers from the problems of overfitting [20, 21]. For the observed data t the Bayes' factor between two models M_1 and M_2 reads:

$$\frac{P(M_1|\tau \leq t \leq \tau + d\tau)}{P(M_2|\tau \leq t \leq \tau + d\tau)} = \underbrace{\frac{p(t|M_1)}{p(t|M_2)}}_{\text{Bayes factor}} \times \frac{P(M_1)}{P(M_2)}, \quad (16)$$

where $P(M_1)$ and $P(M_2)$ are prior distributions associated with each model.

The two likelihoods entering the Bayes' factor can be calculated by integrating over the complete set of parameters as:

$$p(t|M_i) = \int p(t|\theta_i, M_i)p(\theta_i|M_i) d\theta_i, \quad i = \{1, 2\}, \quad (17)$$

where $p(t|\theta_i)$ and its corresponding parameter sets $\theta_i = \{\mu_i, \lambda_i\}$ and the prior $p(\theta_i|M_i)$ depends on whether we use M_1 (pure IG model) or M_2 (mixture IG model) respectively.

The calculation of $p(t|M_1)$ from (17) is fairly straightforward since we assume that bearing is operating under constant rotational speed. For such a case, the prior $p(\theta_1|M_1)$ takes simple form. On the other hand, the calculation of the second marginal $p(t|M_2)$ from (17) depends on the selection of the appropriate prior describing the statistical properties of the rotational speed variations captured with $p(\theta_2|M_2)$. In many cases the integral (17) is intractable. A possible solution is the application of Monte Carlo integration.

5.1. Model specification with Gaussian prior

Setting the prior $p(\theta_2|M_2)$ in (17) to be Gaussian can be regarded as a safe choice in cases when the speed mean value is known but proper prior information about the variation of the rotational speed profile is missing. For such a case the speed fluctuations can be defined as [22]:

$$\delta = d + \varepsilon, \text{ where } \varepsilon \sim \mathcal{N}(0, \sigma_\delta^2), d \geq 0, \delta > 0, \quad (18)$$

where the only hyperparameter θ_2 is the variance σ_δ^2 . The limitation $\delta > 0$ imposes additional limitation on the distribution of ε in (18) i.e. the Gaussian distribution of ε should be truncated so that $\varepsilon > -d$ and it reads [22]:

$$p(\delta) = \frac{1}{\Phi\left(d\sqrt{\frac{\lambda}{\nu}}\right)} \left(\frac{\lambda}{2\pi\nu}\right)^{1/2} \exp\left(-\frac{\lambda(\delta-d)^2}{2\nu}\right), \delta \geq 0, \quad (19)$$

where $\Phi(\cdot)$ is the cumulative function of the standard normal distribution. Using (19) as a prior for the speed fluctuations, the marginal likelihood (17) reduces to (7) and reads:

$$p(t; \lambda, \sigma_\delta, d) = \sqrt{\frac{\lambda}{2\pi t^3(1 + \lambda\sigma_\delta^2 t)}} \exp\left(-\frac{\lambda(dt-1)^2}{2t(1 + \lambda\sigma_\delta^2 t)}\right) \frac{\Phi\left(\frac{d + \lambda\sigma_\delta^2}{|\sigma_\delta|\sqrt{1 + \lambda\sigma_\delta^2 t}}\right)}{\Phi\left(\frac{d}{\sigma_\delta}\right)}. \quad (20)$$

It should be noted that for the special case when $\sigma_\delta = 0$, the mixture inverse Gaussian (20) reduces into its standard form (5).

6. Experiments

The proposed model based on mixture inverse Gaussian distribution of the inter-event times was evaluated using vibration signals acquired from electronically commutated motor with localised bearing fault. In both cases, the observed vibrations were generated under several different speed profiles, according to the model (18) with mean value $d = 38$ Hz. The standard deviation σ_δ changed from 0% up to 10% of the mean speed.

6.1. Experimental setup

The vibration signals, generated by the electronically commutated (EC) motor, were acquired using the test rig shown in Figure 6. The rig consists of a fixed pedestal with rubber dumpers on top of which the test EC motor is positioned. The generated vibrations are measured using two accelerometers positioned on the bearing's sleeves. Both vibration signals were low-pass filtered with cut-off frequency at 22 kHz and sampled at 60 kHz. The faulty bearing was mounted on the EC motor's non-driven end. Seeded fault was introduced on the outer ring by means of electronic discharging machine. The fault was $\sim 2^\circ$ wide and has average surface depth of 30 μm .

The seeded fault can be considered as a severe one. However, as the goal of the experiment is the detection of impact times, such a fault allows straightforward detection of excited impulse responses. Thus enabling sufficiently accurate extraction time intervals between two consecutive impacts.

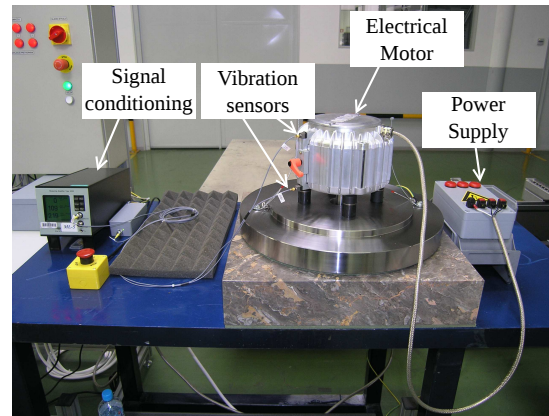


Figure 6: Experimental set up for electronically commutated motors

6.2. Detection of impacts times

The main signal processing step, prior to the application of proposed IG based models, concerns the calculation of the time intervals between two consecutive impacts. In our approach, the detection of impact times was performed using wavelet transform thresholding [23]. Schukin et al. [24] suggested that for signals containing repetitive impulse responses, an optimal detection of impacts can be performed by using mother wavelet that will closely match the underlying vibrational patterns. According to the thorough analysis of Unser and Tafti [25], on the other hand, the crucial parameter for sparse wavelet representation of signals, containing repetitive impulse responses, is the number of vanishing moments of the mother wavelet. Going this way seems less demanding than looking for the “optimal” mother wavelet that will closely match the underlying signal. Therefore, by selecting a wavelet with sufficiently high number of vanishing moments one can sufficiently accurately analyse vibrational patterns containing the impulse responses from the excited eignemodes regardless of their variable form due to the changes of the transmission path. The schematic representation of the impact detection process is shown in Figure 7.

In our approach, the generated vibrations were analyzed using Daubechies 8 mother wavelet [26]. For our particular system such a number of vanishing moments has shown to be sufficient for accurate impulse detection.

6.3. Numerical calculation of the Bayes' factor

Having the impact times t_i the next step is to calculate the Bayes' factor by calculating the marginal distributions (17). The marginal likelihoods were calculated using Monte Carlo integration. Since the

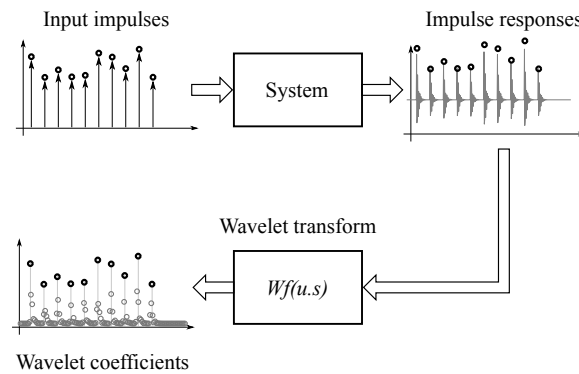


Figure 7: Detection of impact times using wavelet as differential operator

model selection depends on standard deviation σ_δ , the selected prior was the so-called folded non-central t distribution which reads [27]:

$$p(\sigma_\delta) \propto \left(1 + \frac{1}{\gamma} \left(\frac{\sigma_\delta}{A}\right)^2\right)^{-(\gamma+1)/2}, \tag{21}$$

where A is scale parameter and γ represents the degrees of freedom. The prior for the mean value d in (18) was chosen to be uniform in a sufficiently wide interval. The prior for the remaining parameter $\lambda = 1/\sigma^2$ in (3) was also chosen to be uniform in the interval that contains 2% of initial speed fluctuations due to slippage [14].

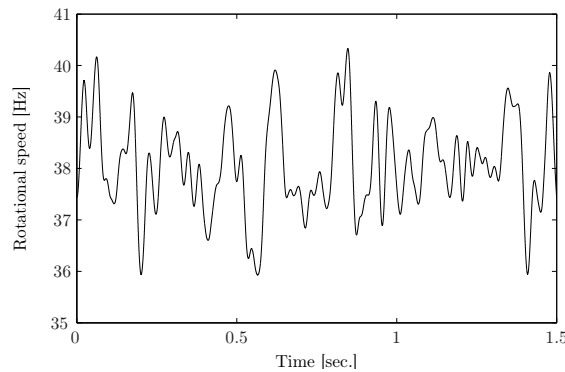


Figure 8: Applied speed fluctuation profile

6.4. Results

One realisation of the speed fluctuations, with $d = 38$ Hz, is shown in Figure 8. The speed fluctuations are smooth but sufficiently fast. Consequently, even during a single bearing revolution the rotational speed varies. The histogram of impact times with the corresponding distributions are shown in Figure 9.

The impact times were extracted using the wavelet analysis of the generated vibrations using Daubechies 8 mother wavelet. Due to the significant fault severity, the detection of the impact times can be performed

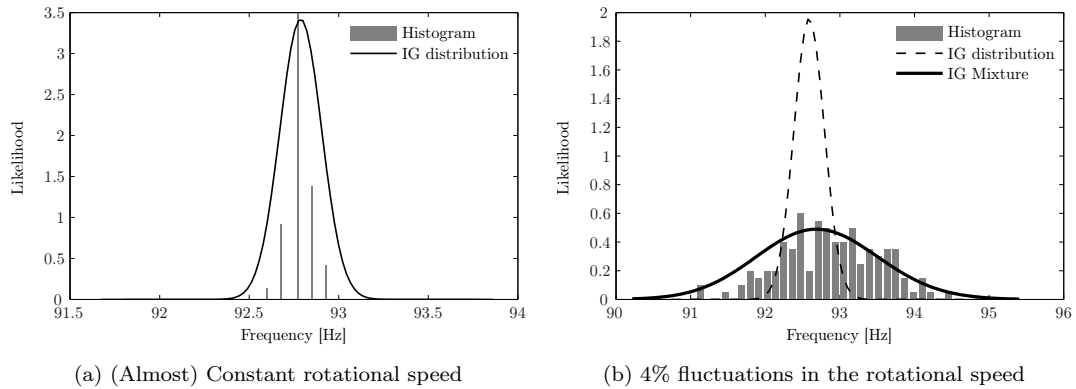


Figure 9: Distribution of impact times

sufficiently accurately. Based on the extracted impact times, for small speed deviations $\sigma_\delta < 0.5\%$ of the mean speed value d , the Bayes' factors (17) overwhelmingly favour simpler model (5) i.e. pure inverse Gaussian distribution of the inter-event times. For speed fluctuations with $\sigma_\delta > 0.5\%$ the Bayes' factors favour mixture inverse Gaussian model for the inter-event times. Changes of the Bayes' factor with respect to the changes in the speed fluctuations σ_δ are shown in Figure 10.

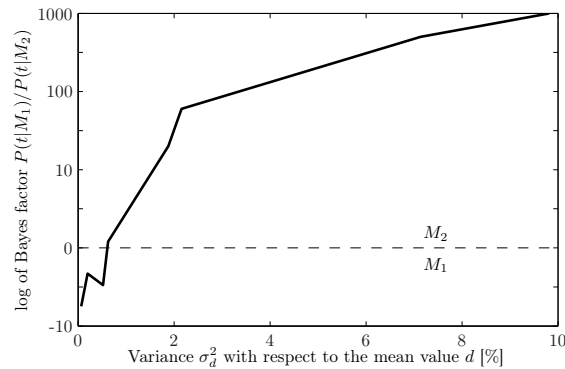


Figure 10: Changes of the Bayes' factors for different σ_δ

Such results are (somewhat) expected since under small speed fluctuations pure inverse Gaussian distribution of the inter-event times sufficiently well describes the observed impact times. At the same time, due to the principle of parsimony, the simpler model is preferred. The cost of more complex model becomes justified when the speed fluctuations become more intensive.

7. Conclusion

The experimental results show that the time occurrences of the vibrational patterns generated by bearings with surface faults can be treated as a realisation of a point process whose inter-event times are distributed according to either pure or inverse Gaussian mixture. The first model is applicable for the special case

when fault bearings operate under constant rotational speed. The model using inverse Gaussian mixture is a general solution applicable also for modelling the impact times of faulty bearings operating under variable rotational speed.

Employing inverse Gaussian distribution for inter-event times resolves several issues present in the currently available models. The most important one is that the proposed model provides a physically sound description of the statistical properties of the inter-event times by using a distribution defined on the interval $[0, \infty)$. Furthermore, the model inherently describes the quasi-cyclostationary characteristics of the impact times under almost constant rotational speed. Finally, by employing the Bayes' factors it is shown that when the speed fluctuations exceed one percent the rotational speed should no longer be regarded as constant.

The proposed model provides a unified description for both single and multiple localised surface bearing faults regardless of the rotational speed. It offers a way for proper statistical analysis of inter-event times of the occurrence of the vibrational patterns under arbitrary speed profiles by specifying the appropriate prior distribution in the Bayes' rule.

Acknowledgment

We like to acknowledge the support of the Slovenian Research Agency through Research Programme P2-0001 and Research Project L2-4160.

Appendix A. Derivation of autocorrelation (14)

Appendix A.1. Probability of consecutive events

For a point process let the probability density of a single event occurring up to time t_1 be $p_1(t_1)$. The probability density $p_k(t_k)$ for k consecutive events occurring up to the time moment t_k reads [18]:

$$p_k(t_k) = \int_0^{t_k} p_{k-1}(t_{k-1})p_1(t_k - t_{k-1})dt_{k-1}. \quad (\text{A.1})$$

The Eq. (A.1) is a convolution of two probability densities defined on the non-negative real line, since both $t_k > 0$ and $t_k > t_{k-1}$. This convolution can be elegantly calculated using the Laplace transform of (A.1) as:

$$p_{L,k}(s) = p_{L,k-1}(s)p_{L,1}(s) = p_{L,1}^k(s), \quad (\text{A.2})$$

where $p_{L,k-1}(s) = \mathcal{L}\{p_{k-1}(t)\}$, $p_{L,1}(s) = \mathcal{L}\{p_1(t)\}$ and $\mathcal{L}\{\cdot\}$ stands for the Laplace transform.

In case of IG inter-event times, $p_{L,1}(t)$ is the Laplace transform of (6) i.e.:

$$p_{L,1}(s) = \exp \left\{ \frac{\nu a}{\sigma^2} \left[1 - \sqrt{1 + 2 \frac{\sigma^2}{\nu^2} s} \right] \right\} \quad (\text{A.3})$$

Calculating then the inverse $\mathcal{L}^{-1}\{p_{L,1}^k(s)\}$ of (A.3) results in [28]:

$$p_k(t) = \frac{ka}{\sigma\sqrt{2\pi t^3}} \exp\left\{-\frac{(\nu t - ka)^2}{2\sigma^2 t}\right\}. \quad (\text{A.4})$$

The obtained result (A.4) has quite intuitive explanation. In (6) the threshold for the Wiener process was set at a . Therefore the time t needed to observe k consecutive crossings has the same distribution as if one elevated the threshold up to ka .

Appendix A.2. Autocorrelation of a point process with IG inter-event distribution

The autocorrelation $R_{xx}(\tau)$ of a (renewal) point process has the following form [18]:

$$R_{xx}(\tau) = \nu\delta(\tau) + \tilde{p}_x(\tau), \quad (\text{A.5})$$

where ν is the “frequency” with which the events occur (firing rate), $\nu\delta(\tau)$ represents the probability of an event occurring at time t and *the same* event occurring in time $t + \tau$, whereas $\tilde{p}_x(\tau)$ represents joint probability density of an event occurring at time t and *another* one occurring at time $t + \tau$. Furthermore, the joint probability of the k th event occurring at time t while the $k + n$ th event occurring at time $t + \tau$ is $p_n(\tau)$. Having this in hand the probability $\tilde{p}_x(\tau)$ becomes a sum of probabilities that an event occurs at time t whereas the n th consecutive event occurs at time $t + \tau$. Hence $\tilde{p}_x(\tau)$ becomes:

$$\tilde{p}_x(\tau) = \nu \sum_{n=1}^{\infty} p_n(\tau). \quad (\text{A.6})$$

Using (A.1) for $p_n(\tau)$, (A.6) becomes

$$\tilde{p}_x(\tau) = \nu p(\tau) + \int_0^{\tau} p(\tau') \tilde{p}_x(\tau - \tau') d\tau'. \quad (\text{A.7})$$

Calculating the Laplace transform of (A.7) transforms it into

$$\tilde{p}_{Lx}(s) = \frac{\nu p_L(s)}{1 - p_L(s)}. \quad (\text{A.8})$$

Substituting (A.3) for $p_L(s)$ and using the final value theorem of the Laplace transform it can be readily shown that

$$\lim_{\tau \rightarrow \infty} R_{xx}(\tau) = \frac{2\sigma^2}{a\nu} < \infty. \quad (\text{A.9})$$

- [1] P. F. Albrecht, J. C. Appiarus, D. K. Shrama, Assesment of the reliability of motors in utility applications, IEEE Transactions of Energy Conversion EC-1 (1986) 39–46.
- [2] M. reliability working group MRWG, Report of Large Motor Reliability Survey of Industrial and Commercial Installations, Part III, IEEE Transactions of Industry Applications IA-23 (1985) 153–158.
- [3] N. Tandon, A. Choudhury, A review of vibration and acoustic measurement methods for the detection of defects in rolling element bearings, Tribology International 32 (1999) 469–480.
- [4] J. Antoni, R. B. Randall, A stochastic model for simulation and diagnostics of rolling element bearings with localized faults, Journal of Vibration and Acoustics 125 (3) (2003) 282–289.

- [5] P. Borghesani, R. Ricci, S. Chatterton, P. Pennacchi, A new procedure for using envelope analysis for rolling element bearing diagnostics in variable operating conditions, *Mechanical Systems and Signal Processing* 38 (1) (2013) 23 – 35.
- [6] P. Boškosi, Đ. Juričić, Detection of bearing faults based on inverse Gaussian mixtures model, in: *Surveillance 7 : international conference*, Chartres Institute of Technology, Chartres, France, 2013.
- [7] D. R. Cox, V. Isham, *Point Processes*, Chapman and Hall, Cambridge, 1980.
- [8] D. Daley, D. Vere-Jones, *An Introduction to the Theory of Point Processes: Elementary Theory and Methods*, vol. 1, Springer-Verlag, New York, second edition edn., 2003.
- [9] M. V. Matthews, W. L. Ellsworth, P. A. Reasenberg, A Brownian Model for Recurrent Earthquakes, *Bulletin of the Seismological Society of America* 92 (6) (2002) 2233–2250.
- [10] E. Schrödinger, Zur Theorie der Fall- und Steigversuche an Teilchen mit Brownscher Bewegung, *Physikalische Zeitschrift* 16 (1915) 289–295.
- [11] J. L. Folks, R. S. Chhikara, The Inverse Gaussian Distribution and Its Statistical Application—A Review, *Journal of the Royal Statistical Society. Series B (Methodological)* 40 (3) (1978) 263–289.
- [12] G. A. Whitmore, Normal-Gamma Mixtures of Inverse Gaussian Distributions, *Scandinavian Journal of Statistics* 13 (3) (1986) 211–220.
- [13] A. F. Desmond, G. R. Chapman, Modelling Task Completion Data with Inverse Gaussian Mixtures, *Journal of the Royal Statistical Society. Series C (Applied Statistics)* 42 (4) (1993) 603–613.
- [14] R. B. Randall, J. Antoni, S. Chobsaard, The relationship between spectral correlation and envelope analysis in the diagnostics of bearing faults and other cyclostationary machine signals, *Mechanical Systems and Signal Processing* 15 (2001) 945 – 962.
- [15] P. Boškosi, Đ. Juričić, Point processes for bearing fault detection under non-stationary operating conditions, in: *Annual Conference of the Prognostics and Health Management Society*, Montreal, QC, Canada, 427–434, 2011.
- [16] P. Boškosi, Đ. Juričić, Modeling localized bearing faults using inverse Gaussian mixtures, in: *V: Annual Conference on Prognostics and Health Management Society*, PHM Society, New Orleans, USA, 2013.
- [17] R. Chhikara, J. L. Folks, *The Inverse Gaussian Distribution, Theory, Methodology, and Applications*, vol. 59, Marcel Dekker, New York, 1989.
- [18] C. van Vreeswijk, Analysis of Parallel Spike Trains, vol. 7 of *Springer Series in Computational Neuroscience*, chap. Stochastic Models of Spike Trains, Springer, 3–20, 2010.
- [19] J. Antoni, R. B. Randall, Differential Diagnosis of Gear and Bearing Faults, *Journal of Vibration and Acoustics* 124 (2) (2002) 165–171.
- [20] P. Berkes, J. Fiser, A frequentist two-sample test based on Bayesian model selection, *ArXiv e-prints* .
- [21] D. J. C. MacKay, *Information Theory, Inference, and Learning Algorithms*, Cambridge University Press, 4th edn., 2005.
- [22] A. F. Desmond, Z. L. Yang, Score tests for inverse Gaussian mixtures, *Applied Stochastic Models in Business and Industry* 27 (6) (2011) 633–648, ISSN 1526-4025, doi:10.1002/asmb.876, URL <http://dx.doi.org/10.1002/asmb.876>.
- [23] W. J. Staszewski, Wavelet based compression and feature selection for vibration analysis, *Journal of Sound and Vibration* 211 (1998) 735 – 760.
- [24] E. Schukin, R. Zamaraev, L. Schukin, The optimisation of wavelet transform for the impulse analysis in vibration signals, *Mechanical Systems and Signal Processing* 18 (6) (2004) 1315—1333.
- [25] M. Unser, P. Tafti, Stochastic models for sparse and piecewise-smooth signals, *IEEE Transactions on Signal Processing* PP (99) (2010) 1–1.
- [26] I. Daubechies, *Ten Lectures on Wavelets*, SIAM, Philadelphia, 1992.
- [27] A. Gelman, Prior distributions for variance parameters in hierarchical models, *Bayesian Analysis* 1 (3) (2006) 515—533.
- [28] M. C. K. Tweedie, Statistical Properties of Inverse Gaussian Distributions. I, *The Annals of Mathematical Statistics* 28 (2)

(1957) 362–377.